AMSE JOURNALS-2016-Series: Modelling A; Vol. 89; N°1; pp 118-129
Submitted July 2016; Revised Oct. 15, 2016, Accepted Dec. 10, 2016

Dynamic Performance Analysis of the Induction Motor Drive Fed by Current-Source Based on Ansoft

Zhen Guo[1,2 *], Jiasheng Zhang[1], Changming Zheng[1] and Zhenchuan Sun[1]

[1]College of Information and Control Engineering, China University of Petroleum, Qingdao, 266580, China (qs2004b@163.com)

[2]College of automation engineering, Qingdao University of Technology, Qingdao 266520, China

Abstract:

The dynamic performance of induction motor fed by current-source are analyzed in this paper based on Ansoft. The theory of symmetrical components is used to derive the fundamental formula of induction motor fed by current-source and the co-simulation method combined Ansoft/Maxwell 2D and Ansoft/Simplorer is studied in detail. The characteristics of induction motor fed by current-source in different working condition are analyzed. The results indicate the changes in the magnetic field and operating performance variations of the induction motor fed by current-source compare with that fed by voltage-source. The conclusions provide a reference for theoretical research of induction motor body and optimal design of its control system.

Keywords: Co- simulation model, finite element analysis, current-source, induction motor

1. Introduction

In the variable speed drive systems, induction motors are widely used in industrial application [1,2]. Induction motor drives employ mostly a voltage-source inverter (VSI) topology. However, its application is restricted by poor load current limitation capability, dynamic response retardation and four-quadrant operation limitation. Contrarily, the current source inverter (CSI) is a strong candidate for induction motor drive systems due to its inherent advantages such as perfect over-current ability, good dynamic response and regenerative capability [3,4]. These features make the CSI fed induction motor drive more and more attractive in medium to high power application. A typical configuration of three-phase CSI is shown in Fig.1.

More exploitation have been done to the CSI fed induction motor drive system [5,6,7,8]. However, most of the researches showed little concerns to the operating characteristics variations of induction motor fed by current-source. When the induction motor is fed by voltage-source, the stator voltage is constant and the stator current is forced to fluctuate. When the induction motor is fed by current-source, the stator current is maintained constant and the output stator voltage is forced to change with the load. In fact, the operation performance and magnetic field of the induction motor fed by current-source vary greatly compared with that fed by voltage-source. This paper presents the changes in the magnetic field and operating performance variations of the induction motor fed by current-source compare with that fed by voltage-source which provides reference for further study on electromagnetic theory and mechanical characteristics of CSI fed induction motor drive.

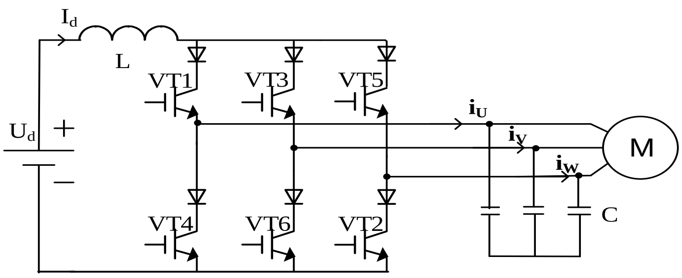

Fig.1. Configuration of three-phase CSI topology

2. The Basic Equations of Induction Motor Fed by Current-Source with Symmetrical Components Method

The motor can be described by fourth-order matrix equation in *α-β* reference frame as follows:

$$\begin{bmatrix} \dot{U}_{s\alpha} \\ \dot{U}_{s\beta} \\ 0 \\ 0 \end{bmatrix} = \begin{bmatrix} R_s + j\omega_s L_{s\sigma} & 0 & j\omega_s M_{sr\sigma} & 0 \\ 0 & R_s + j\omega_s L_{s\sigma} & 0 & j\omega_s M_{sr\sigma} \\ j\omega_s M_{sr\sigma} & (\omega_s - \omega_{sl}) M_{sr\sigma} & R_r + j\omega_s L_{r\sigma} & (\omega_s - \omega_{sl}) L_{r\sigma} \\ -(\omega_s - \omega_{sl}) M_{sr\sigma} & j\omega_s M_{sr\sigma} & (\omega_s - \omega_{sl}) L_{r\sigma} & R_r + j\omega_s L_{r\sigma} \end{bmatrix} \begin{bmatrix} \dot{I}_{s\alpha} \\ \dot{I}_{s\beta} \\ \dot{I}_{r\alpha} \\ \dot{I}_{r\beta} \end{bmatrix} \quad (1)$$

and the impedance matrix in *α-β* reference frame can be expressed as

$$[Z]_{\alpha\beta} = \begin{bmatrix} R_s + j\omega_s L_{so} & 0 & j\omega_s M_{sro} & 0 \\ 0 & R_s + j\omega_s L_{so} & 0 & j\omega_s M_{sro} \\ j\omega_s M_{sro} & (\omega_s - \omega_{sl}) M_{sro} & R_r + j\omega_s L_{ro} & (\omega_s - \omega_{sl}) L_{ro} \\ -(\omega_s - \omega_{sl}) M_{sro} & j\omega_s M_{sro} & (\omega_s - \omega_{sl}) L_{ro} & R_r + j\omega_s L_{ro} \end{bmatrix} \tag{2}$$

Assume that the stator current is unsymmetrical $\dot{I}_{s\alpha}$, $\dot{I}_{s\beta}$ can be replaced by the positive sequence component $\dot{I}_P$ and negative sequence component $\dot{I}_N$. They are related by the following equation:

$$\begin{cases} \dot{I}_{s\alpha} = \dot{I}_P + \dot{I}_N \\ \dot{I}_{s\beta} = -j\,\dot{I}_P + j\,\dot{I}_N \end{cases} \tag{3}$$

Similarly, the relation of the rotor current with symmetrical component method is described as follows:

$$\begin{bmatrix} \dot{I}_{r\alpha} \\ \dot{I}_{r\beta} \end{bmatrix} = \begin{bmatrix} 1 & 1 \\ -j & j \end{bmatrix} \begin{bmatrix} \dot{I}_f \\ \dot{I}_b \end{bmatrix} \tag{4}$$

Impedance matrix $[Z]_{pn}$ in symmetrical component coordinates results from $[Z]_{\alpha\beta}$, so

$$[Z]_{pn} = \begin{bmatrix} R_s + j\omega_s L_{so} & 0 & j\omega_s M_{sro} & 0 \\ 0 & R_s + j\omega_s L_{so} & 0 & j\omega_s M_{sro} \\ j(\omega_s - \omega_r) M_{sro} & 0 & R_r + j\omega_s L_{ro} & 0 \\ 0 & j(\omega_s + \omega_r) M_{sro} & 0 & R_r + j(\omega_s + \omega_r) L_{ro} \end{bmatrix} \tag{5}$$

The voltage equation of the induction motor in symmetrical coordinates can be expressed as

$$\begin{bmatrix} \dot{U}_P \\ \dot{U}_N \\ \dot{U}_f \\ \dot{U}_b \end{bmatrix} = \begin{bmatrix} R_s + j\omega_s L_{so} & 0 & j\omega_s M_{sro} & 0 \\ 0 & R_s + j\omega_s L_{so} & 0 & j\omega_s M_{sro} \\ j(\omega_s - \omega_r) M_{sro} & 0 & R_r + j\omega_s L_{ro} & 0 \\ 0 & j(\omega_s + \omega_r) M_{sro} & 0 & R_r + j(\omega_s + \omega_r) L_{ro} \end{bmatrix} \begin{bmatrix} \dot{I}_P \\ \dot{I}_N \\ \dot{I}_f \\ \dot{I}_b \end{bmatrix} \tag{6}$$

The positive sequence component of the stator and the rotor can be an independent coordinate. Similarly, the negative sequence component can be too. The second line and the third line of equation (6) are interchanged, so equation (6) is now transformed into equation (7)

$$\begin{bmatrix} \dot{U}_P \\ \dot{U}_f \\ \dot{U}_N \\ \dot{U}_b \end{bmatrix} = \begin{bmatrix} R_s + j\omega_s L_{so} & j\omega_s M_{sro} & 0 & 0 \\ j(\omega_s - \omega_r) M_{sro} & R_r + j(\omega_s - \omega_r) L_{ro} & 0 & 0 \\ 0 & 0 & R_s + j\omega_s & j\omega_s L_{ro} \\ 0 & 0 & j(\omega_s + \omega_r) M_{sro} & R_r + j(\omega_s + \omega_r) \end{bmatrix} \begin{bmatrix} \dot{I}_P \\ \dot{I}_f \\ \dot{I}_N \\ \dot{I}_b \end{bmatrix} \tag{7}$$

The rotor voltages of the squirrel-cage induction motor is zero, so $\dot{U}_f = \dot{U}_b = 0$ .When the stator current is symmetrical, the negative component $\dot{I}_N = \dot{I}_b = 0$, equation (7) can be changed into

$$\begin{bmatrix} \dot{U}_P \\ 0 \end{bmatrix} = \begin{bmatrix} R_s + j\omega_s L_{so} & j\omega_s M_{sro} \\ j(\omega_s - \omega_r) M_{sro} & R_r + j(\omega_s - \omega_r) L_{ro} \end{bmatrix} \begin{bmatrix} \dot{I}_P \\ \dot{I}_f \end{bmatrix} \tag{8}$$

so

$$\begin{cases} \dot{U}_P = (R_s + j\omega_s L_{so}) \dot{I}_P + j\omega_s M_{sro} \dot{I}_f \\ 0 = j\omega_s M_{sro} \dot{I}_P + (R_r + j(\omega_s - \omega_r) L_{ro}) \dot{I}_f \end{cases} \tag{9}$$

When the stator $\dot{I}_P$ is a known value, the rotor current is as follows:

$$\dot{I}_f = -\frac{j\omega_s M_{sro}}{R_r + j(\omega_s - \omega_r) L_{ro}} \dot{I}_P = -\frac{j\omega_s M_{sro}}{R_r + j\omega_{sl} L_{ro}} \dot{I}_P \tag{10}$$

Then the stator voltage can be written as

$$\begin{aligned} \dot{U}_P &= (R_s + j\omega_s L_{so}) \dot{I}_P + j\omega_s M_{sro} \dot{I}_f \\ &= (R_s + j\omega_s L_{so}) \dot{I}_P + \left(-\frac{j\omega_s M_{sro}}{R_r + j\omega_{sl} L_{ro}}\right) \dot{I}_P \end{aligned} \tag{11}$$

And

$$\dot{I}_p = \sqrt{3}\, \dot{I}_A \tag{12}$$

The equation of the electromagnetic torque, output power and the stator flux can be derived based on the equations from (9) to (12).

3. The establishment of finite element model

Analysis and simulation modeling techniques in induction motors can be classified in two categories. One is electrical parameter model, the other is to build the motor model by using motor design software. The method of the electrical parameter model can observe the electrical characteristics of the induction motor, but the internal magnetic field of the motor cannot be obtained. By using motor design software to establish the motor model can get part of the electrical characteristics and the internal magnetic field, but it is unfitted to the complex electrical system. So the co-simulation method is explored in this paper which meet the demand of the complex the drive system. The Ansoft/Maxwell 2D and Ansoft/Simplorer are used to build model of the induction motor fed by current-source to explore the characteristics variation compare with that fed by voltage-source. An four-pole induction motor is presented in this paper. The parameters of tested motor are listed in Table I.

Table I. Parameters for tested motor

Parameters	Values
Rated Shaft Power	11 KW
Rated Phase Voltage	380 V
Rated Frequency	50Hz
Synchronous Speed	1500r/min
Number of The Pole Pairs	2
Number of Stator Slots	36
Number of Rotor Slots	26
Outer Diameter of Stator	260mm
Inner Diameter of Stator	170mm
Outer Diameter of Rotor	169mm
Inner Diameter of Rotor	60mm
Core Length	155mm

In accordance with the model requirements, the material properties of the motor are set including stator winding, stator core and rotor core and other parts of the motor. Because of the two dimensional analysis of the motor, the vector magnetic field in Z direction is set to 0. In the finite element model of induction motor, no-load speed and rated speed of the motor are set 1500 rpm and 1462 rpm respectively. According to the mechanical parameters of the motor，the finite element model is created in Ansoft /RMxprt which is shown in Fig.2.

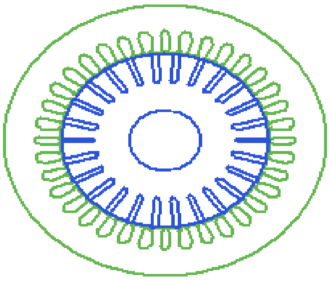

Fig.2. Finite element model of tested motor

4. The co-simulation method combined Ansoft/Maxwell 2D and Ansoft/Simplorer

Importing the finite element model and building the peripheral circuit and relevant load in Ansoft/simplorer, the co-simulation system is built which is shown in Fig.3. The Phase A in and Phase A out of the motor represent both ends of the A phase winding, Phase B in and Phase B out represent the ends of the B phase winding and Phase C in and Phase C out represent both ends of the C phase winding. I_1, I_2 and I_3 are three-phase symmetrical current-source. The A, B, C three-phase in ports are connected to the three-phase current-source. The A, B, C three-phase out ports are connected together to form the star structure of the stator winding. MotionSetup1_in and MotionSetup1_out ports are motor mechanical port. The inertia MASS_ROT1 and load torque F_ROT1 are connected to MotionSetup1_out. The load torque are added by using STEP1 and STEP2. MotionSetup1_in is grounded.

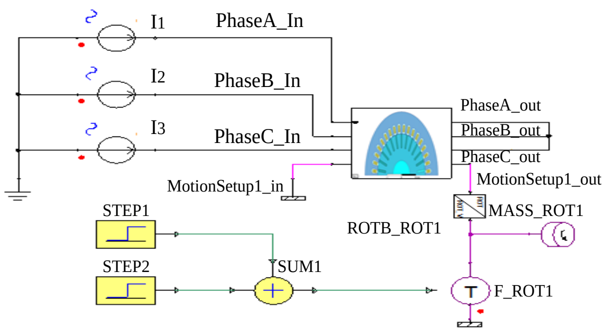

Fig.3. The co-simulation model of the induction motor fed by current-source

5. Simulation results and analysis

When the induction motor is fed by current-source, the input is the stator three-phase currents and the stator currents are constant when load is varying. At start-up, the induction motor under no load is fed by rated current at 50HZ. A rated load is 70N.m which is applied after start-up transient time 4s. The simulation results are shown in Fig.4(a) including the stator currents wave, stator voltages wave, electromagnetic torque wave and motor speed wave.

To compare the characteristics difference of induction motor fed by between current-source and voltage-source, the waves of induction motor fed by voltage-source are presented in Fig.4(b) including stator voltages wave, stator currents wave, electromagnetic torque wave and motor speed wave. It can be seen from the Fig.4(b) that the input of induction motor is stator three-phase rated voltages instead of three-phase rated currents. A sudden load 70N.m is applied after start-up transient time 0.5s. Fig.4 shows that when the induction motor is fed by current-source, the stator currents are maintained constant irrespective of load variation and the output stator voltages are forced to fluctuate. When the induction motor is fed by voltage-source, the stator voltages are constant and the stator currents are forced to change. The starting torque of the induction motor fed by rated current is lower than that fed by the rated voltage.

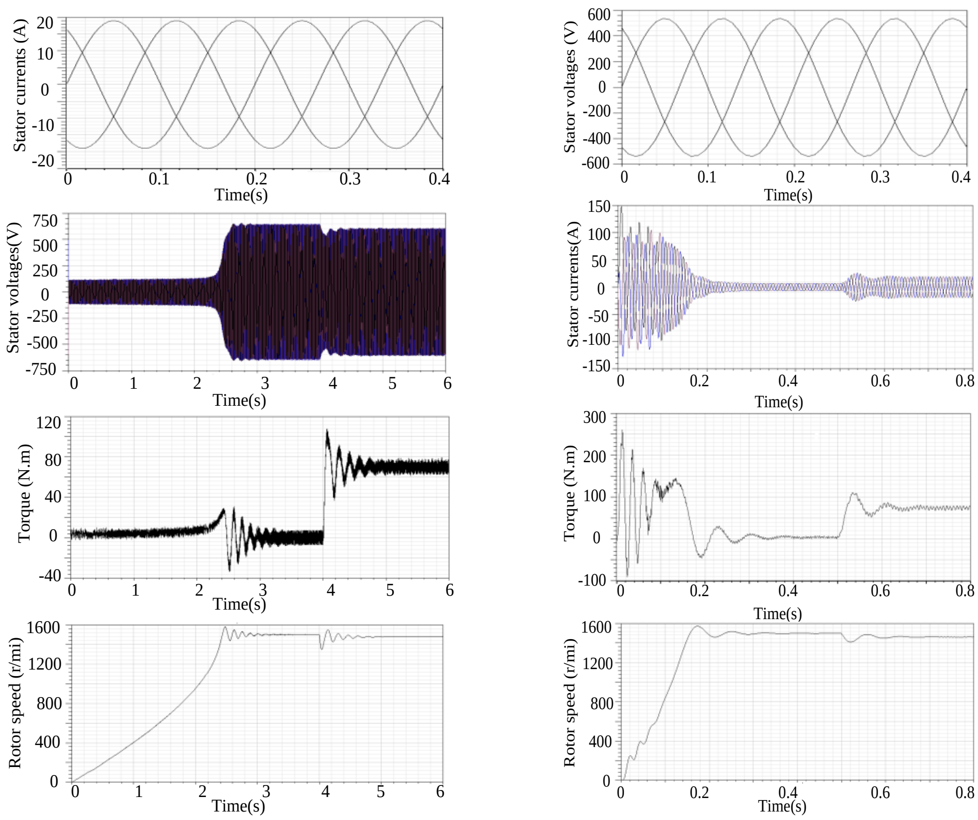

(a) Fed by current-source (b) Fed by voltage-source

Fig.4. The simulated waveforms at 50HZ of the induction motor

The co-simulation model of the motor can not only present the electrical characteristics waveforms of the system, but also can observe the changes of the magnetic field of the motor during the operation. Two cases are given to present the magnetic field distribution difference of the induction motor between fed by current-source and by voltage source. One is in start process under no-load, the other is in steady state under rated load. Due to the symmetry, only one half-structure of the induction motor is shown in Fig. 5 and Fig.6. Magnetic field distribution of the induction motor fed by current-source and by voltage source at 53rpm speed during the start process are shown in Fig. 5(a) and Fig.5(b) separately. When the induction motor is fed by rated voltage-source, the starting current of the motor is larger than the rated current. However, the stator current of the motor fed by current-source is maintained constant. Therefore, it can be seen from Fig.5 that the magnetic flux intensity of the induction motor fed by current-source is lower than that fed by voltage-source during the start process of the motor. There is no severe magnetic saturation phenomenon in Fig.5(a), however, the magnetic saturation of silicon steel sheet is both obvious and serious in Fig.5(b). The Fig.6 presents the magnetic field distribution of the induction motor fed by current-source and by voltage source at 1462 rpm speed with the rated load in steady state. When the motor is in stable operation under rated load, the stator current whenever the motor is fed by current-source or by voltage-source are both rated current, so there is little difference between Fig.6(a) and Fig.6(b).

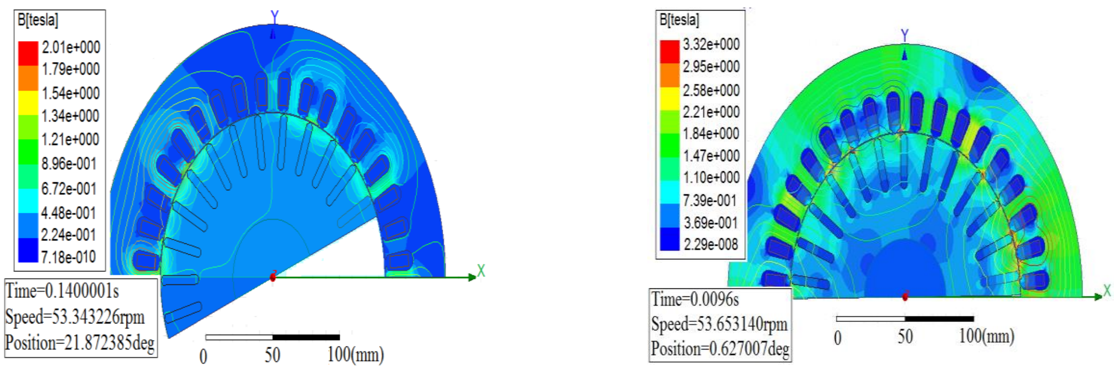

(a) Fed by current-source (b)Fed by voltage-source

Fig.5. Magnetic field distribution of tested motor at 53rpm speed

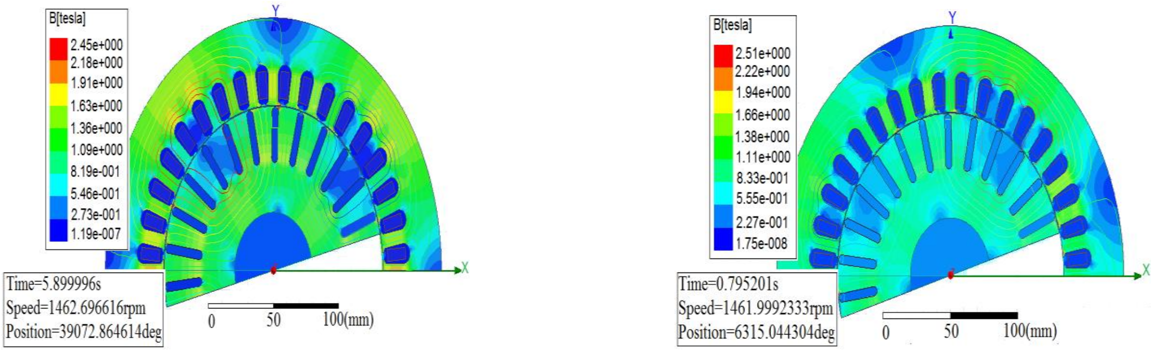

(a) Fed by current-source (b) Fed by voltage-source

Fig.6. Magnetic field distribution of tested motor at 1462rpm speed

6. Conclusion

The dynamic performance of the induction motor fed by current-source are analyzed in this paper. The co-simulation system combined Ansoft/Maxwell 2D and Ansoft/Simplorer is built. The simulation results indicate the changes not only in the operating performance but also in magnetic field of the induction motor fed by current-source compare with that fed by voltage-source. The conclusions provide a reference for theoretical research of induction motor body and optimal design of its control system.

Nomenclature

R_s , R_r stator , rotor resistance

L_{so} , L_{ro} stator self-inductance, rotor self-inductance

M_{sro} mutual inductance of the motor

$\dot{U}_{s\alpha}$, $\dot{U}_{s\beta}$ α-axis and β-axis components of stator voltages

$\dot{I}_{s\alpha}$, $\dot{I}_{s\beta}$ α- axis and β-axis components of stator current

$\dot{I}_{r\alpha}$, $\dot{I}_{r\beta}$ α- axis and β-axis components of rotor current

$\dot{I}_P$, $\dot{I}_N$ positive sequence and negative sequence components of stator current in symmetrical coordinates

$\dot{I}_f$, $\dot{I}_b$ positive sequence and negative sequence components of rotor current in symmetrical coordinates

$\dot{I}_A$ A phase of stator current

ω_s , ω_r , ω_{sl} synchronous , rotor and slip speed in electrical radians/second.

$[Z]_{\alpha\beta}, [Z]_{pn}$ αβ-axis and symmetrical coordinate impedance matrix

$\dot{U}_P$, $\dot{U}_f$ positive sequence component of stator voltage and rotor voltage in symmetrical coordinates

$\dot{U}_b$, $\dot{U}_N$ negative sequence component of stator voltage and rotor voltage in symmetrical coordinates

References

[1] Bimal K.Bose, Modern power electronics and AC drives.[M]. Beijing : China machine press, 2013.

[2] P. Enjeti, P. Ziogas, and J. Lindsay, "A current source PWM inverter with instantaneous current control capability," IEEE Trans. Ind Applicat., vol.27, pp.643–893, May/June 1991.

[3] BinWu, High-power converters and AC Drives. Piscataway, NJ: Wiley-IEEE Press, 2006.

[4] Behrooz Mirafzal and Nabeel A.O. Demerdash, "A Nonlinear Controllerfor Current Source Inverter Induction Motor Drive Systems," IEEE Trans. On Electric Machines and Drives, vol.3 No. 2, pp.1491 - 1497, 2003.

[5] A. Nabae, I. Takahasi, and H. Akasi, "A Neutral Point Clamped PWM Inverter," in Conf. Rec. IEEE-IAS Annu. Meeting, 1980, pp.530–536.

[6] P. M. Bhagwat and V. R. Stefanovic, "Generalized Structure of a Multilevel PWM Inverter," IEEE Trans.Ind. Applicat, vol. IA-19, pp.1057–1069, Nov./Dec.1983.

[7] R. J. Kerkman, "Twenty years of PWM AC Drives when Secondary Issues Become Primary Concerns," in Proc. IECON'96 Conf., Taipei, Taiwan, R.O.C., pp. LVII–LXIII. Aug. 1996.

[8] Seyed Hamid Shahalami, “Special Proposed Hysteresis Control Method of Current Source Inverter Asynchronous Drives”, IEEE 1st Power Electronic & Drive Systems &Technologies Conference, pp.235-242, 2010.

[9] Aleksandar Nikolic, Borislav Jeftenic, “Different Methods for Direct Torque Control of Induction Motor,” Wseas Transactions on Circuits and Systems, Volume 7, pp.739 - 748, 2008.

[10] Morawiec, Zbigniew Krzeminski, Arkadiusz Lewicki, “Voltage multiscalar control of induction machine supplied by current source converter,” IEEE, pp.3119-3124, 2010.

[11] J. Espinoza and G. Jos, “Current-source converter on-line pattern generator switching frequency minimization,” IEEE Trans. Ind. Electron.,vol.44, pp.198–206, Apr. 1997.

[12] A. R. Beig and V. T. Ranganathan, “A novel CSI-fed induction motor drive,” IEEE Trans. Power Electron., vol.21, no. 4, pp.1073– 1082, Jul. 2006.

[13] A. M. Trzynadlowski, N. Patriciu, F. Blaabjerg, and J. K.Pedersen, “A Hybrid, Current Source/Voltage Source Power Inverter Circuit,” IEEE Trans. Power Electron., vol.16, no. 6, pp.866-871, Nov. 2001.

[14] R. Emery and J. Eugene, “Harmonic Losses in LCI fed Synchronous Motors,” IEEE Trans. Ind. Appl., vol. 38, no. 4, pp. 948–954, Jul./Aug. 2002.

[15] D. Banerjee, “Load commutated SCR current source inverter fed induction motor drive with sinusoidal motor voltage and current,” Ph.D. dissertation, Dept. Electr. Eng., Ind. Inst. Sci. (IISc), Bengaluru, India, Jul. 2008.

[16] B.Wu, S. Dewan, and G. Slemon, “PWM CSI Inverter for Induction Motor Drives,” IEEE Trans. Ind. Applicat., vol.28, pp.317–325, Jan./Feb. 1992.

[17] A. G. Yepes, F. D. Freijedo, J. Doval-Gandoy, O. Lopez, J. Malvar, and P. Fernandez-Comesana, “Effects of discretization methods on the performance of resonant controllers,” IEEE Trans. Power Electron., vol.25, no. 7, pp. 1692–1712, Jul. 2010.

[18] J. Hu and B. Wu, “New integration algorithms for estimating motor flux over a wide speed range,” IEEE Trans. Power Electron., vol. 13, no. 5,pp. 969–977, Sep. 1998.

[19] Seyed Hamid Shahalami, “Special Proposed Hysteresis Control Method of Current Source

Inverter Asynchronous Drives," IEEE 1st Power Electronic & Drive Systems &Technologies Conference, pp.235-242, 2010.

[20]B. Bahrani, S. Kenzelmann, and A. Rufer, "Multivariable-PI-based DQ current control of voltage source converters with superior axes decoupling capability," IEEE Trans. Ind. Electron., vol. 58, no. 7, pp.3016–3026, Jul. 2011.

[21]Yu Xiong, Danjiang Chen, Xin Yang, Changsheng Hu and ZhongchaoZhang, "Analysis and Experimentation of A New Three-phase Multilevel Current-Source Inverter," IEEE Trans. On Telecommunications Energy Conference, Vol.1, pp.548-551, 2004.

[22]Pramod Agarwal, V.K. Verma and A.K. Pandey,"Performance Evaluation of a Self-commutating CSI-fed Induction Motor Drive for Different Operating Conditions, IETE Journal of Research, Vol.54, Issue 4, pp.227-238,July/Aug. 2008.

[23]Adrian Schiop and Daniel Trip, "Analysis of the Trapezoidal Modulation for Current Source Inverters," IEEE Trans. On Signals, Circuits and Systems, Vol.2, pp. 1-4, 2007.

[24] P. Agarwal and V.K. Verma, "Parameter Coordination of Microcomputer Controlled CSI-fed Induction Motor Drive", IE (I) Journal – EL, Vol.88, pp.25-34, December 2007.

[25]Hak-Jun Lee, Sungho Jung and Seung-Ki Sul, "Analysis and Experimentation of A New Three-phase Multilevel Current-Source Inverter," IEEE Trans. On Telecommunications Energy Conference, Vol.1, pp.1364-1370, 2011.

[26]Pramod Agarwal, A.K. Pandey and V.K. Verma, "Performance Investigation of Modified Self-commutated CSI-fed Induction Motor Drive, Asian Power Electronics Journal, Vol.3, No.1, pp.21-29, Sept 2009.